Final version available in Journal of Applied Physics 119, 205303 (2016); https://doi.org/10.1063/1.4952709

Interfacial characterization of Al-Al thermocompression bonds

N. Malik,[1,2,a)] P. A. Carvalho,[3] E. Poppe[2] and T. G. Finstad[1]

[1]*Centre for Materials Science and Nanotechnology, University of Oslo, PO Box 1032, Blindern, N-0315 Oslo, Norway*

[2]*SINTEF ICT, Department of Microsystems and Nanotechnology, PO Box 124 Blindern, N-0314 Oslo, Norway*

[3]*SINTEF Materials and Chemistry, Department of Materials and Nanotechnology, PO Box 124 Blindern, N-0314 Oslo, Norway*

[a)]nishantmalik1987@gmail.com

ABSTRACT

Interfaces formed by Al-Al thermocompression bonding were studied by transmission electron microscopy. Si wafer pairs were bonded using Al films deposited on Si or SiO_2 as intermediate bonding media. A bond force of 36 or 60 kN at bonding temperatures ranging from 400–550 °C was applied for a duration of 60 min. Differences in bonded interfaces of 200 µm wide sealing frames were investigated. Interface having voids was observed for bonding with 36 kN at 400 °C for Al deposited both on Si and on SiO_2. However, the dicing yield was 33 % for Al on Si and 98 % for Al on SiO_2, attesting for the higher quality of the latter bonds. Both a bond force of 60 kN applied at 400 °C and a bond force of 36 kN applied at 550 °C resulted in completely bonded frames with dicing yields of, respectively, 100 and 96 %. A high density of long dislocations in the Al grains was observed for the 60 kN case, while the higher temperature resulted in grain boundary rotation away from the original Al-Al interface towards more stable configurations. Possible bonding mechanisms and reasons for the large difference in bonding quality of the Al films deposited on Si or SiO_2 are discussed.

I. INTRODUCTION

Unlike integrated circuits (ICs), micro electromechanical systems (MEMS) often have a moving part that requires a vacuum environment for reliable functioning. MEMS packaging can account for 40 to 70 % of the overall system cost.[1] Wafer level packaging (WLP) provides a solution to encapsulate MEMS at wafer level and integrate with other system components, reducing the expense of post-foundry operations.[2]

There is a wide range of methods available for wafer level sealing of MEMS devices[3]. Metal thermocompression bonding has attracted increased interest,[4] in which two metal surface are bonded together by the continuous application of pressure and temperature. Metals offer certain advantages over non-metals as metals are much less permeable to gases than other intermediate layers used for bonding and hence offer the advantage of smaller device size because of the narrower frames.[5-7] The required width may also depend upon the completeness of bonding which will change for different metals and processing parameters. Metal seals can provide mechanical bonding and electrical connections in the same fabrication step. Moreover, metals demonstrate good electrical and thermal conductivity. Metal thermocompression bonding have been demonstrated for 3D integration[8], packaging of micro-valves[9], IR sensors[10] and accelerometers[11].

The metals mainly used for bonding include Al,[12-14] Au[15] and Cu.[16] Au and Cu can be bonded at relatively low temperatures compared to Al as Al forms a native oxide on its surface on exposure to the air, this oxide is mechanically very strong. Still, Al-Al thermocompression bonding has recently attracted much interest contrarily to Au- and Cu-based bonding as it can be easily integrated in complementary metal–oxide–semiconductor (CMOS) processing routes. Al

deposition as well as etching techniques are well evolved and can be patterned with standard IC processes while, Au and Cu can increase complexity or cost of MEMS processing.

Successful Al-Al thermocompression bonding has previously been reported. Martin et al. bonded seal rings seal rings of width 4–90 μm at 445 °C by applying a bond pressure of 30 MPa.[12] A shear strength of 740 g was reported for 30 μm wide rings, which was equal to the shear strength of a 150 μm wide glass frit bond. Bond force was said be to the key metric in this report. A systematic study of varying bond force (9, 14 and 18 kN) and Cu impurity content (0–4 %) in Al was performed by Yun et al..[13] The bonding temperature was kept constant at 450 °C. Increasing bond force showed an increase in the yield and shear strength. The yield was slightly higher for pure Al, but the Al with 4% Cu resulted in the highest shear strength. Dragoi et al. investigated the effect of varying the bonding temperature (400–550 °C), time (1–4 h) and environment (N_2 and forming gas) on the quality of Al thermocompression bonds.[14] The different bonding environment and time did not affect the bond quality, while a trend of increasing interfacial adhesion energy with increasing bonding temperature was observed.

Al-Al thermocompression bonding at varying ranges of bonding temperature (300–550 °C), pressure (34–114 MPa) and time (15–60 min) have previously been reported by our group.[17-19] It was found that Al films sputtered on SiO_2 can be bonded at lower temperatures than those sputtered directly on Si wafers.[18] We also found that higher quality bonding in terms of dicing yield and bond strength can be achieved by increasing the bonding temperature and/or bond force.[17] In the current work, we use transmission electron microscopy (TEM) to investigate bonded interfaces realized with Al deposited on Si or on SiO_2 to explore possible reasons leading to differences in dicing yield. The impact of increasing the bond force and bond temperature on the resulting bond interface is also investigated.

II. EXPERIMENTAL

Four wafer laminates were fabricated by Al-Al thermocompression bonding using 200 μm wide sealing frames. Two laminates, named Si400 and Si550, consisting of 1 μm thick Al films sputter deposited directly on Si (001) wafers, were bonded with a bond force of 36 kN at 400 and 550 °C, respectively, which correspond to Al homologous temperatures of 0.72 and 0.88. The two other laminates, named Ox400 and Ox400-60, consisting of Al films sputter deposited on thermal (amorphous) SiO_2 formed on Si (001) wafers. The bonding was performed by pressing the bonding surface on the wafers against each other applying an initial bond force of 1 kN, then the bonding temperature was raised to the desired value and after temperature stabilization, the desired bond force was applied. The bonding temperatures were 400 °C or 550 °C and applied bond forces were 36 or 60 kN, respectively (details described elsewhere).[14] For these forces the estimated contact pressure on the 200 μm wide frame is ~ 26 and 43 MPa.[19] The sputtering parameters were identical; only the deposition surface and bonding conditions differed. A list of the samples, corresponding bonding parameters, resulting dicing yields and bond strengths can be found in Table 1. For each laminate, the dicing yield is defined as the percentage of dies on a wafer that do not delaminate during dicing. The bond strength was measured with pull tests at room temperature using non-delaminated dies (details described elsewhere).[14]

Only non-delaminated dies were selected for TEM investigation. Sample preparation was carried out by focused ion beam using a JIB 4500 Multi Beam JEOL instrument employing Ga beams. The die was previously diced into half to expose the cross-section of the bonded interface, as shown in Fig. 1. A thin slice of the bonded interface was cut, transferred by a micro-manipulator to a copper lift-out grid and subsequently polished down to a thickness <100 nm.

Conventional bright-field transmission electron microscopy (bright-field TEM), high resolution transmission electron microscopy (HRTEM), scanning transmission electron microscopy (STEM) and high resolution scanning transmission electron microscopy (HRSTEM) in high angle annular dark field (HAADF) mode, with a convergence angle of 22 mrad and a collection angle of 76-200 mrad, were used to investigate the cross-section of the bonded interfaces using a probe corrected Titan™ G2 60-300 FEI instrument equipped with energy-dispersive X-ray spectroscopy (EDS) to determine the elemental composition of the bonded films.

III. RESULTS

A general view of the bonded interface of sample Si400 is shown in Fig. 2. Diffraction contrast in bright-field TEM imaging (Fig. 2 (a)) reveals a straight Al-Al interface configuration and Al grains with a height comparable to the film thickness (1 μm) and diameters ranging between 0.5 and 1.5 μm. In addition, long-range strain fields at the Si/Al interface can be seen (annotated in Fig. 2 (a)). Figure 2 (b) and (c) present, respectively, an STEM/HAADF image and an EDS oxygen map of the same interface. Discontinuous oxide patches can be seen. Voids are also observed at the interface. Roughly, half of the interface appears to consist of voids in the shown image. The maximum gap between the two opposing Al surfaces was found to be in the order of 50 nm. Native oxide layers were found at the bonding interface.

Figure 3 presents bright-field TEM images of the bonded interface of sample Ox400. In Fig. 3 (a) and (b) a straight Al-Al interface is seen and the height of the Al grains is comparable to the film thickness (1 μm) with diameters ranging between 1.0 and 2.5 μm. Long-range stress fields at the Si-SiO_2 interface are also seen. It was estimated by STEM/HAADF imaging of the

interface that about half of the interface consisted of voids and that the maximum gap was on the order of 70 nm (Fig. 3 (c)). The mottled contrast present in the Al grains for both imaging methods suggests the presence of dislocations resulting from plastic deformation.

Figure 4 shows TEM images of the bonded interface in sample Ox400-60. It is seen from Fig. 4 (a) that the Al-Al interface is straight and the height of the Al grains is comparable to the film thickness (1 μm), while their in-plane size ranges from 1.0 to 3.0 μm. A high density of long dislocation lines is present in the Al grains indicating plastic deformation. Dislocation loops and stacking faults in the Al thin film were also detected as shown in the insets. Figure 4 (b) presents a HRTEM image of the Al-Al bonded interface for the same sample. The EDS oxygen map of the region in (c) is shown in (d). The interface exhibits a broken Al oxide layer.

Figure 5 shows TEM images of the bonded interface in sample Si550. From Fig. 5 (a) it is seen that the height of the Al grains is essentially given by the film thickness (0.6 μm) while their in-plane size ranges from 1.0 to 2.5 μm. A high density of dislocation loops is present in the Al grains indicating plastic deformation. Unlike the frames bonded at 400 °C, the Si550 sample presented a zigzag interface resulting from grain boundary (GB) migration. Long-range stress fields at the Al/Si interface are annotated in Fig. 5 (a). The STEM image in Fig. 5 (b) shows a small void/gap in the apparently well bonded interface. The corresponding EDS oxygen map in Fig. 5 (c) reveals the presence of a broken Al oxide layer at the interface.

IV. DISCUSSION

In this discussion we first address the effect of the native oxide layer on bonding. Then we argue on the origin of the bonding gaps and reflect on grain size, crystallographic texture and stress fields. Based on these interpretations we discuss the bonding difference between Al films grown directly on Si substrates and films grown on SiO_2 interlayers. Finally, we address the effect of increasing force or temperature on eliminating gaps and obtaining complete bonding at the Al-Al interface.

Exposure of a clean Al surface to air results in the quick growth ($\ll$1sec)[20] of a mechanically strong and chemically inert oxide layer that reaches a self-limiting thickness of 3–4 nm. Oxide layers were expected on the sputtered Al films since they have been exposed to air before loading into the wafer bonder. The native oxide hinders the direct contact of the two opposing surfaces, and needs to be broken up to allow bonding of the metal by solid state welding. Previous work suggested that this requires relatively high temperatures and/or bond forces[18] and, in fact, broken oxide layers are distinctively observed at the interfaces in Fig. 4 (d) and 5 (c) obtained, respectively, with a bond force of 60 kN and at a temperature of 550 °C.

Voids/gaps at the Al-Al interfaces can be seen in samples Si400 and Ox400 (Figs. 2 (b) and 3 (c) respectively). The maximum gap height is much larger than the as-deposited roughness of Al films on Si or SiO_2 (<5 nm).[21] It is also much larger than the roughness of films deposited with identical parameters as here and annealed to 400 °C.[21] Thus the initial film roughness is not responsible for the observed behavior, however, Al films develop hillocks when annealed in mechanically unconstrained conditions.[22] In the present case the bonded wafers were pressed against each other with a force of 1 kN during heating.[18] If this pressure was not sufficient to

suppress the hillock formation, then the hillocks could be an obstacle to full contact between the wafers and promote voids. Hillock formation can be prevented depositing Ti or TiW prior to Al.[23] Still, as observed for the Ox400 sample, incomplete bonding may result in high dicing yield (Fig. 3 and Table 1). From this behavior it is reasonable to deduct the following: i) acceptable bonding for practical applications may contain voids; ii) the potential of lowest permeability and very narrow bonding frames for a sealing metal bond may not be reached unless bonding parameters are optimized for each case. Clearly, for vacuum sealing, voids are undesirable and can be suppressed with higher forces and/or by increasing the bonding temperature.

According to previous electron backscattered diffraction (EBSD) studies reported by Malik et al.,[21] the Al films deposited on Si (001) exhibit an average grain size *(d*) and distribution width (±) similar to that of films deposited on amorphous SiO_2, respectively, 0.9 ± 1.5 and 0.9 ± 1.6 µm, although a significantly stronger (111) texture is observed for the former. Mechanically unconstrained annealing at 400 °C results in considerable grain growth for both Al on Si (001) and Al on SiO_2[21] (albeit less pronounced for the former, with d = 2.7 ± 4.6 µm and d = 3.3 ± 5.4 µm, respectively). While grain growth is expected to be affected by the applied pressure, the larger grain size of Al here in the Ox400 sample compared to the Si400 one (Fig. 2 (a) and Fig. 3 (a)) is in line with the previous observations. It is interesting to notice the straight interfaces in the samples bonded at 400 °C (Figs. 2 and 3); as there is no indication of mass transfer across the original interface in the TEM micrographs, we may assume that grain growth occurred parallel to the surface. We interpret this as an indication of lamellar growth, meaning that for these bonding conditions the grains in the two mating films grow separately.

It is worth mentioning the dominating (111) texture of the present Al films and the known anisotropic mechanical behavior of Al single crystals. The yield stress for single crystal Al (at

room temperature) under uniaxial stress is much higher along the [111] direction than along other crystallographic directions (for example a factor 2 difference between [111] and [100]).[24] This is related to a lower number of available {111}<110> slip systems for the configuration resulting from applying the stress perpendicular to (111). A strong (111) texture, such as the present case, might thus require a higher applied stresses to initiate plastic deformation compared to random crystallographic orientations. However, the fact that at higher temperatures glide may occur in additional planes, such as {110} and {100},[25-27] the effect not least the hillocks constitute a difficulty in the analysis, but the argument about enhanced mechanical strength for the (111) may hold.

The stress fields characteristically present both at the Al-Si and SiO_2-Si interfaces (Fig. 2 (a) and Fig. 3 (a)) can originate from thermal expansion differences. Indeed, the linear thermal expansion coefficient of Al is one order of magnitude larger than that of Si which is four times higher than that of amorphous SiO_2. As such, compressive stresses parallel to the interfaces develop in the Al films upon cooling from the relaxed state at higher temperature, and these residual stresses are more pronounced for Al-SiO_2 than for Al-Si. We believe that these residual stresses play an important role in the initiation/propagation of cracks since a higher fraction of cohesive Si fractures has been observed with increasing bonding temperature with little change in bond strength.[28]

We will now discuss the reasons behind the different bonding quality for Al deposited directly on the Si substrate compared to Al deposited on an intermediate SiO_2 layer. Although the Al-Al interfaces shown in Fig.2 (a) and in Fig. 3 (a) are qualitatively similar, one should bear in mind that there has been a statistically biased pre-selection of the dies from laminate Si400 by the dicing process. Two hypotheses fall naturally from the discussion to justify the better

bonding of the Ox400 samples; i) a small but significant difference in local plasticity exists between the two types of laminates, favoring solid state welding in the Ox400 case, and/or ii) the residual thermal stresses affected the dicing yield. A close inspection to the contrast differences of the Al grains reveals a higher density of dislocations in the Ox400 sample (Fig. 3 (b)) which is in agreement with the observed differences in bonding behavior. The less pronounced (111) texture of the $Si/SiO_2/Al$ system as well as the progressively larger grain size suggests a larger plasticity for these Al films. According to the Hall-Petch dependence of yield stress with grain size, the yield strength increases with decreasing grain size as $d^{-0.5}$ where d is the grain size.[29] Thus, the lower yield stress and concomitant higher local plasticity of the Al films deposited on SiO_2 may have promoted the rupture of the native aluminum oxide layers favoring metallic welding and causing the large difference in dicing yield for a bonding force of 36 kN at 400 °C (Table 1).

The TEM images of the sample bonded at 400 °C with a force of 60 kN show a high density of long dislocations and stress accumulated in the Al grains (Fig. 4 (a) and (b)). The higher bonding pressure promotes dislocation slip and thus plastic deformation which breaks the oxide layers and overcomes surface asperities by increasing the number of atoms in contact. Grain boundary sliding could also have been contributed in reducing the voids at the interface. The result is a straight but completely bonded interface.

The effect of increasing the bonding temperature from 400 °C to 550 °C can clearly be seen in Fig. 5. The zigzag Al-Al interface shows interlocked grains across the two Al layers. The grain growth is not lamellar as observed for the lower bonding temperature, i.e., here the GB network is converging towards the low energy 120° triple joint between grain boundaries, that are characteristic equilibrium configurations. The network then acts as if the two layers were one

sole medium. A large net mass transfer across the original interface has taken place during bonding. At this high temperature (homologous temperature of 0.88) the metal should be extremely soft and diffusive creep is dominating the deformation mechanisms. The discontinuous line of oxide at the zigzag GBs shows that the broken Al native oxide tends to form clusters/precipitates at the grain boundaries during bonding.[30] Only minor gaps are present at the interface (Fig. 5 (c)). These may not yet be closed or can originate from surface contamination or from defects existing on the Al surface prior to bonding.

Figure 6 shows the schematic of the bonded interface produced at: a) low bonding temperature and pressure, b) high pressure and low temperature, c) low pressure and high temperature. The low/high threshold for bonding temperature or pressure varies with the metal used in sealing and with grain size and preferred crystallographic orientation. In a) the dicing yield may be low if an intimate contact between the two metal surfaces has not been generated. In b) a straight and completely bonded interface forms without significant voids/gaps, as the applied high pressure brings the metal surfaces into close contact by plastic deformation. When the structure is bonded at higher temperature the interface between the two surfaces develops zig-zag grain boundary, as shown in c) due to diffusive creep.

V. CONCLUSIONS

Al-Al interfaces bonded by thermocompression were investigated for different bonding conditions by means of TEM. The bonding Al film was either deposited directly on the Si wafer or on an oxidized Si wafer. Laminates were produced by bonding of structured Si wafers to plain Si wafers at temperatures of 400 and 550 °C applying bond forces of 36 or 60 kN for a duration of 60 min. The results show incomplete bonded interfaces for a temperature of 400 °C and a

force of 36 kN; with the SiO_2 laminate showing a dicing yield of 98 % while only 33 % of the dies remained bonded after dicing the Si-only laminate. A difference in local plasticity and residual thermal stress are believed to be responsible for the difference in the dicing yield. These results show that, in practice, acceptable bonding may contain voids and be incomplete. Complete bonding was realized at 400 °C by applying a 60 kN bond force, which induced a high density of long dislocations in the bonded Al films. Complete bonding was also achieved at 550 °C by applying a 36 kN bond force, which resulted in reorientation of the interface grain boundaries.

ACKNOWLEDGMENTS

Financial support from The Research Council of Norway through the project MSENS (Contract No. 210601/O30) and NBRIX (Contract No. 247781/O30) is gratefully acknowledged. The authors wish to thank Kari Schjølberg-Henriksen and Maaike M. Visser Taklo from SINTEF ICT for fruitful discussions and Asbjørn Ulvestad at UiO for ion milling of the TEM samples.

REFERENCES

[1] R. Pelzer, H. Kirchberger, and P. Kettner, in *6th international conference on Electronic packaging technology (ICEPT)* (Shenzhen, China, 2005), p. 1.

[2] E. Masayoshi, Journal of Micromechanics and Microengineering **18,** 073001 (2008).

[3] P. Ramm, J. J. Q. Lu, and M. M. V. Taklo, *Handbook of Wafer Bonding* (Wiley, 2012).

[4] J. Froemel, M. Baum, M. Wiemer, F. Roscher, M. Haubold, C. Jia, and T. Gessner, in *16th International Solid-State Sensors, Actuators and Microsystems Conference (TRANSDUCERS)* (Beijing, China, 2011), p. 990.

[5] R. Fraux and J. Baron, in *3D Packaging* (i-Micronews Media, 2011), p. 24.

[6] S. Farrens, in *International Wafer-Level Packaging Conference* (San Jose, CA 2008).

[7] S. Costello and M. P. Y. Desmulliez, *Hermeticity Testing of MEMS and Microelectronic Packages* (Artech House, 2013).

[8] J. Fan and C. S. Tan, *Low Temperature Wafer-Level Metal Thermo-Compression Bonding Technology for 3D Integration* (2012).

[9] I. Chakraborty, W. C. Tang, D. P. Bame, and T. K. Tang, Sensors and Actuators A: Physical **83,** 188 (2000).

[10] D. Xu, E. Jing, B. Xiong, and Y. Wang, IEEE Transactions on Advanced Packaging **33,** 904 (2010).

[11] C. H. Yun, J. R. Martin, T. Chen, and D. Davis, in *MEMS Wafer-Level Packaging with Conductive Vias and Wafer Bonding*, 2007, p. 2091.

[12] J. Martin, in *Wafer capping of MEMS with fab-friendly metals*, 2007, p. 64630M.

[13] C. H. Yun, J. Martin, L. Chen, and T. J. Frey, ECS Transactions **16,** 117 (2008).

[14] V. Dragoi, G. Mittendorfer, J. Burggraf, and M. Wimplinger, ECS Transactions **33,** 27 (2010).

[15] M. M. V. Taklo, P. Storås, K. Schjølberg-Henriksen, H. K. Hasting, and H. Jakobsen, Journal of Micromechanics and Microengineering **14,** 884 (2004).

[16] A. Fan, A. Rahman, and R. Reif, Electrochemical and Solid-State Letters **2,** 534 (1999).

[17] N. Malik, K. Schjølberg-Henriksen, E. Poppe, M. M. V. Taklo, and T. G. Finstad, Sensors and Actuators A: Physical **211,** 115 (2014).

[18] N. Malik, K. Schjølberg-Henriksen, E. Poppe, M. M. V. Taklo, and T. G. Finstad, Journal of Micromechanics and Microengineering **25,** 035025 (2015).

[19] N. Malik, E. Poppe, K. Schjølberg-Henriksen, M. M. V. Taklo, and T. G. Finstad, ECS Journal of Solid State Science and Technology **4,** P251 (2015).

[20] J. Evertsson, F. Bertram, F. Zhang, L. Rullik, L. R. Merte, M. Shipilin, M. Soldemo, S. Ahmadi, N. Vinogradov, F. Carlà, J. Weissenrieder, M. Göthelid, J. Pan, A. Mikkelsen, J. O. Nilsson, and E. Lundgren, Applied Surface Science **349,** 826 (2015).

[21] N. Malik, V. Venkatachalapathy, K. Schjølberg-Henriksen, E. Poppe, M. M. V. Taklo, and T. G. Finstad, in *WaferBond'15* (Braunschweig, Germany, 2015).

[22] S.-J. Hwang, W. D. Nix, and Y.-C. Joo, Acta Materialia **55,** 5297 (2007).

[23] C. D. Graas, MRS Online Proceedings Library Archive **260,** null (1992).

[24] U. F. Kocks, Acta Metallurgica **8,** 345 (1960).

[25] J.-L. Martin and C. D., Zeitschrift für Metallkunde **84,** 867 (1993).

[26] C. Maurice and J. H. Driver, Acta Materialia **45,** 4627 (1997).

[27] F. Perocheau and J. H. Driver, International Journal of Plasticity **18,** 185 (2002).

[28] M. Nishant, S.-H. Kari, U. P. Erik, M. V. T. Maaike, and G. F. Terje, Journal of Micromechanics and Microengineering **25,** 035025 (2015).

[29] S. Khamsuk, N. Park, S. Gao, D. Terada, H. Adachi, and N. Tsuji, Materials Transactions **55,** 106 (2014).

[30] T. Kárpáti, A. E. Pap, G. Radnóczi, B. Beke, I. Bársony, and P. Fürjes, Journal of Micromechanics and Microengineering **25,** 075009 (2015).

LIST OF TABLES

TABLE I. Bonding parameters of all 4 bonded laminates. All laminates were bonded for duration of 60 min. Dicing yield of each laminate and bond strength, as estimated by pull testing of 12 individual dies from each laminate is taken from elsewhere.[18]

FIGURE CAPTIONS

FIG. 1. Cross-sectional schematic of the bonded dies. The top wafer is the flat Si wafer bonded to a structured wafer with bond frames. (a) Top and bottom wafer with Al deposited directly on Si. The sketch represents the cross-section from the bonded laminate Si400 and Si550. (b) Top and bottom wafer with a layer of SiO_2 underneath bonding Al. The sketch represents the cross-section from the bonded laminate Ox300, Ox400 and Ox400-60.

FIG. 2. Bonded interface in sample Si400, the laminate was bonded applying a force of 36 kN at 400 °C for 60 min. (a) Bright-field TEM image. (b) STEM/HAADF image. (c) EDS oxygen map.

FIG. 3. Bonded interface in sample Ox400, the laminate was bonded applying a force of 36 kN at 400 °C for 60 min. (a) Bright-field TEM image. (b) Bright-field TEM image showing local deformation in the Al film. (c) STEM/HAADF image of the Al-Al interface.

FIG. 4. Bonded interface in sample Ox400-60, the laminate was bonded applying a force of 60 kN at 400 °C for 60 min. (a) Bright-field TEM image showing a high density of dislocations in the Al grains. (b) HRTEM image showing the presence of stacking faults and dislocation loops. (c) STEM/HAADF image showing the bonded Al-Al interface. (d) EDS oxygen map corresponding to (c).

FIG. 5. Bonded interface in sample Si550, the laminate was bonded applying a force of 36 kN at 550 °C for 60 min. (a) Bright-field TEM image. (b) STEM/HAADF image showing the interface between two Al grains. The top grain presents a low-index zone axis parallel to the electron beam, while the bottom one is not in Bragg condition; this generates the strong diffraction contrast differences observed. (c) EDS oxygen map.

FIG. 6. Schematic grain structure of the bonded Al-Al interface for different bonding parameters: (a) lower bonding temperature and pressure, b) lower bonding temperature and higher pressure (c) higher bonding temperature and lower pressure.

TABLES

TABLE I. Bonding parameters of all 4 bonded laminates. All laminates were bonded for duration of 60 min. Dicing yield of each laminate and bond strength, as estimated by pull testing of 12 individual dies from each laminate is taken from elsewhere.[18]

Laminate ID	**SiO_2 layer**	**Bond force [kN]**	**Bonding temperature [°C]**	**Dicing yield [%]**	**Bond Strength [MPa]**
Si400	No	36	400	33	27
Ox400	Yes	36	400	98	32
Ox400-60	Yes	60	400	100	60
Si550	No	36	550	96	25

FIGURES

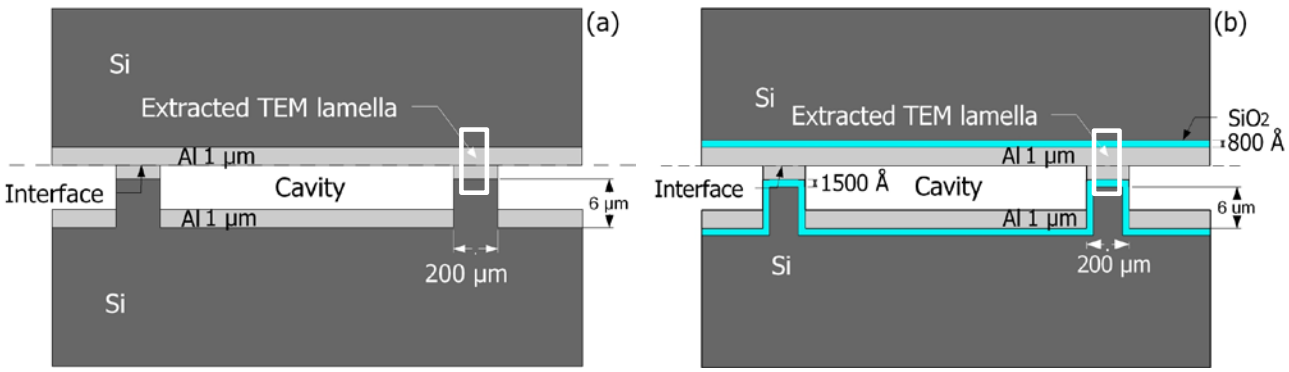

FIG. 1. Cross-sectional schematic of the bonded dies. The top wafer is the flat Si wafer bonded to a structured wafer with bond frames. (a) Top and bottom wafer with Al deposited directly on Si. The sketch represents the cross-section from the bonded laminate Si400 and Si550. (b) Top and bottom wafer with a layer of SiO_2 underneath bonding Al. The sketch represents the cross-section from the bonded laminate Ox400 and Ox400-60.

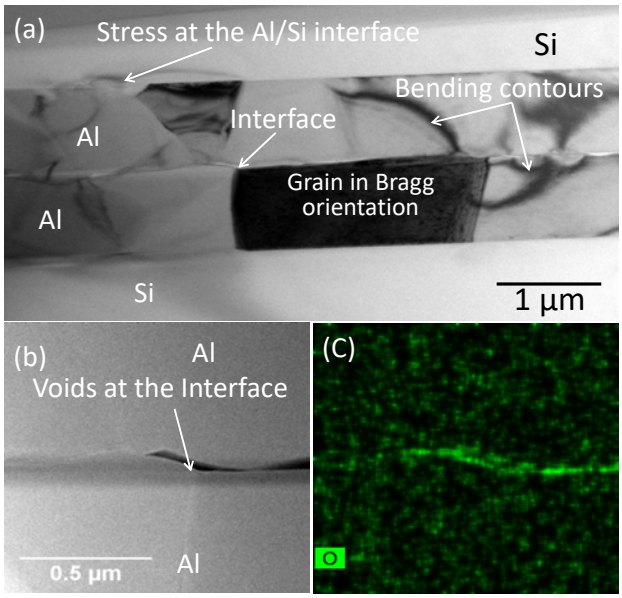

FIG. 2. Bonded interface in sample Si400, the laminate was bonded applying a force of 36 kN at 400 °C for 60 min. (a) Bright-field TEM image. (b) STEM/HAADF image. (c) EDS oxygen map.

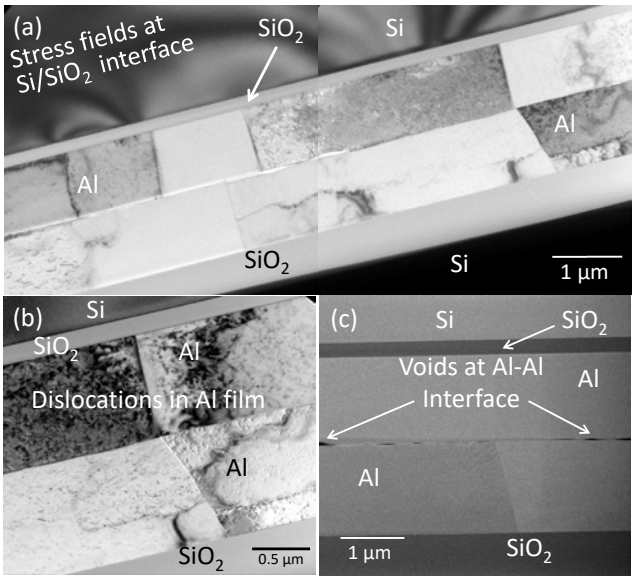

FIG. 3. Bonded interface in sample Ox400, the laminate was bonded applying a force of 36 kN at 400 °C for 60 min. (a) Bright-field TEM image. (b) Bright-field TEM image showing local deformation in the Al film. (c) STEM/HAADF image of the Al-Al interface.

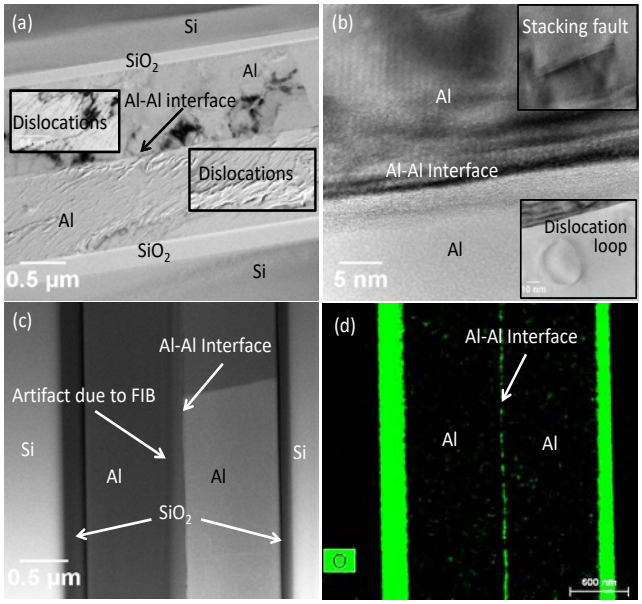

FIG. 4. Bonded interface in sample Ox400-60, the laminate was bonded applying a force of 60 kN at 400 °C for 60 min. (a) Bright-field TEM image showing a high density of dislocations in the Al grains. (b) HRTEM image showing the presence of stacking faults and dislocation loops. (c) STEM/HAADF image showing the bonded Al-Al interface. (d) EDS oxygen map corresponding to (c).

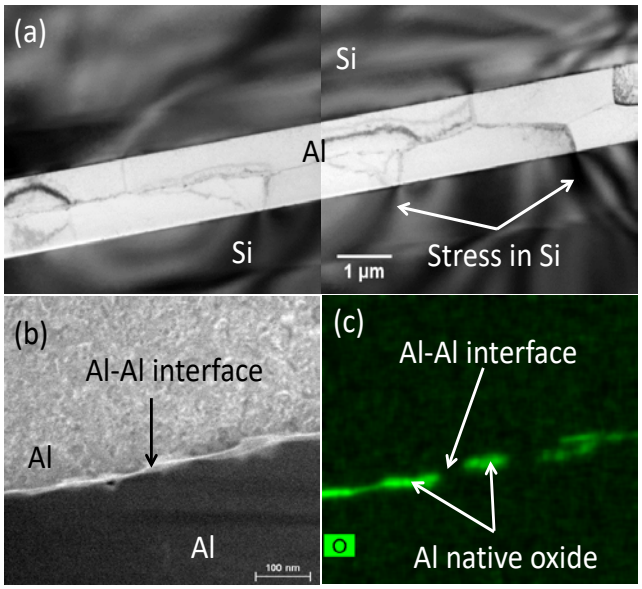

FIG. 5. Bonded interface in sample Si550, the laminate was bonded applying a force of 36 kN at 550 °C for 60 min. (a) Bright-field TEM image. (b) STEM/HAADF image showing the interface between two Al grains. The top grain presents a low-index zone axis parallel to the electron beam, while the bottom one is not in Bragg condition; this generates the strong diffraction contrast differences observed. (c) EDS oxygen map.

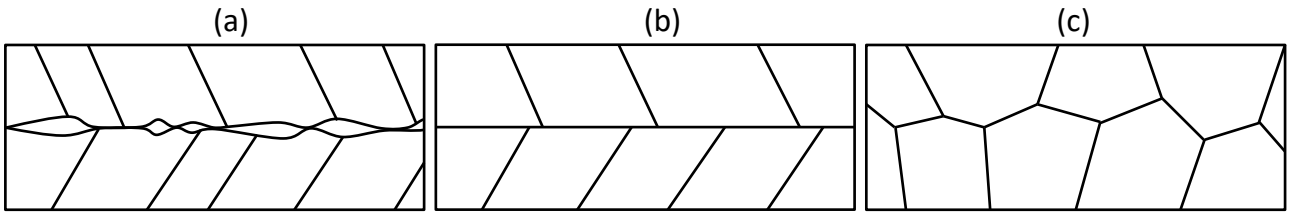

FIG. 6. Schematic grain structure of the bonded Al-Al interface for different bonding parameters: (a) lower bonding temperature and pressure, b) lower bonding temperature and higher pressure (c) higher bonding temperature and lower pressure.